Complete Series of Monohalogenated Isoreticular Metal–Organic Frameworks: Synthesis and the Importance of Activation Method

5 AUTHORS, INCLUDING:

Scott T. Meek
Pixie Scientific
10 PUBLICATIONS   **647** CITATIONS

SEE PROFILE

John Perry IV
University of Limerick
21 PUBLICATIONS   **1,405** CITATIONS

SEE PROFILE

Mark D Allendorf
Sandia National Laboratories
**212** PUBLICATIONS   **8,310** CITATIONS

SEE PROFILE

Complete Series of Monohalogenated Isoreticular Metal−Organic Frameworks: Synthesis and the Importance of Activation Method

Scott T. Meek,[†] John J. Perry IV,[†] Stephanie L. Teich-McGoldrick,[‡] Jeffery A. Greathouse,[‡] and Mark D. Allendorf*,[†]

[†]Sandia National Laboratories, P.O. Box 969, Livermore, California 94551, United States
[‡]Sandia National Laboratories, P.O. Box 5800, Albuquerque, New Mexico 87185, United States

S Supporting Information

ABSTRACT: A series of four IRMOFs with -F, -Cl, -Br, and -I terephthalate linkers was synthesized and characterized with respect to crystal structure, surface area, and nitrogen gas sorption. The activation of these materials was systematically evaluated, using several solvent-exchange methods and supercritical CO_2 drying. The results demonstrate a strong dependence of surface area on the activation method used. Materials with surface areas comparable to predicted values were achieved, considerably improving upon previously reported values for IRMOF-2 and its -I variant. Finally, ambient-temperature nitrogen adsorption isotherms were measured. These data clearly demonstrate that the adsorption of a weakly interacting gas can be improved by increasing linker polarizability, confirming previous speculation in the literature.
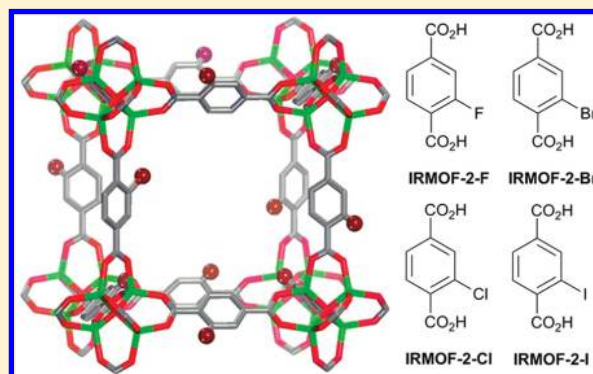
Metal−organic frameworks, which are hybrid lattices of organic electron donors and metal cations, have attracted much attention over the past decade, with applications[1] including gas storage[2] and separation,[3] drug delivery,[4] catalysis,[5] electronics,[6] and sensing.[7] These compounds can exhibit extremely high apparent surface areas, exceeding 10 000 m^2/g (Langmuir) for some materials,[8] as well as low density and thermal stability. Their synthetic flexibility, however, sets them apart from other microporous materials, such as zeolites, activated carbon, and aerogels.

Tailoring the pore environment of a MOF is crucial for controlling its interactions with adsorbates, which ultimately will enable it to be optimized for a particular application. The properties of these materials may be tuned by either modifying the organic linker, exchanging the metal ion, or altering the coordination environment through the introduction of open-metal sites. As a result, one can vary the size and shape of the pores, or modify the functional groups present that interact with the adsorbate. For the effects of these changes to be fully realized, MOFs must be carefully activated after synthesis to ensure that the pores are not occluded with solvent or residual linkers and that the framework has not collapsed. While activation is a crucial step in MOF preparation, few systematic studies of activation conditions have been reported.[9,10]

The addition of polarizable functional groups to the MOF pore environment is expected to increase the strength of the interaction between the framework and guest species,[11] but no systematic studies of this effect appear in the literature. Because their polarizability increases with increasing atomic size, the halogens (fluorine, chlorine, bromine, and iodine) represent a straightforward means of probing the effects of polarizability on adsorbate−MOF interactions. Currently, no isostructural series of MOFs exist with systematic halogen replacement. MOFs having -F,[12−14] -Cl,[12,15,16] -Br,[11,17,18] and -I[19,20] functionalities are known. In addition, a series of Cu-terephthalate MOFs for polymer catalysis with -F, -Cl, and -Br replacement was previously described;[21] however, no surface areas or adsorption isotherms for these compounds were reported. The IRMOF series is ideal for determining the effects of halogenation, and thus polarizability, on adsorbate−framework interactions due to their relative ease of synthesis and extensive data in the literature. Herein we report the synthesis and activation of IRMOF-2[11] variants in which -Br has been replaced with -F, -Cl, and -I (Figure 1) and demonstrate that increasing the polarizability of the MOF pore increases the uptake of N_2 at room temperature.

We obtained the IRMOF-2-X series by synthesizing the -F and -Cl terephthalic acid linkers via oxidation of 3-fluoro- and 3-chloro-4-methylbenzoic acid with $KMnO_4$.[22] Iodoterephthalic acid was synthesized by converting aminoterephthalic acid to a diazonium salt, followed by quenching with KI.[23] The MOFs were prepared using standard solvothermal methods: the terephthalic acid linker (0.8 mmol) and $Zn(NO_3)_2 \cdot 6H_2O$ (2.8 mmol) were mixed in N,N'-diethylformamide, sealed in a jar, and heated at 95 °C for 18−48 h (see Supporting Information for detailed procedures). The PXRD patterns for these compounds (Figure 2) match those predicted for the crystal structure of IRMOF-2 reported
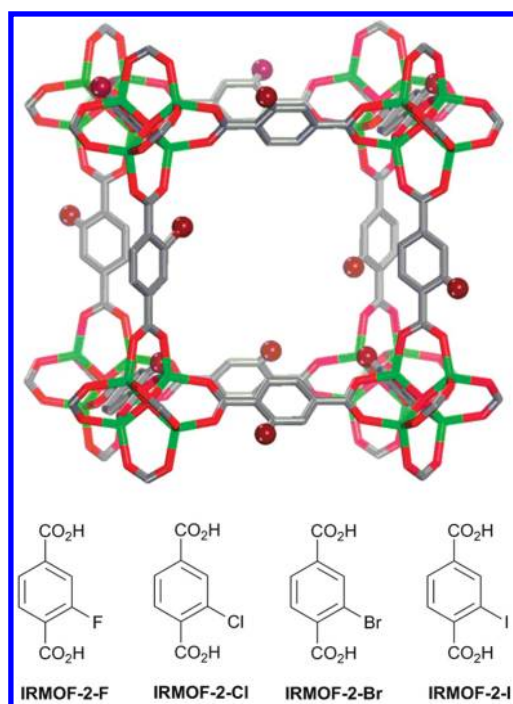
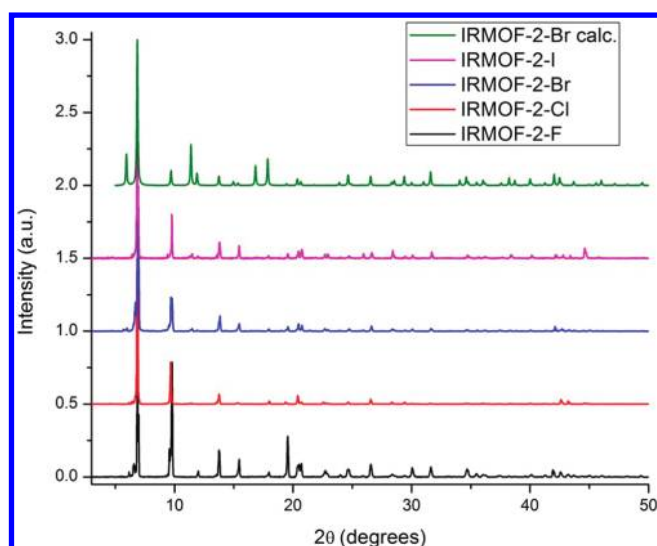**Figure 1.** IRMOF-2 and its -F, -Cl, and -I variants.

Figure 2. PXRD patterns for IRMOF-2-F, IRMOF-2-Cl, IRMOF-2-Br, and IRMOF-2-I, as well as a pattern for IRMOF-2-Br calculated from its published crystal structure.

Table 1. BET Surface Areas^a of Halogenated MOFs

MOF	lit.	calc^b	DMF^c	CHCl$_3^c$	CH$_2$Cl$_2^c$	SC CO$_2^c$
IRMOF-2-F		3172	2503	3133	2879	594
IRMOF-2-Cl		3077	1312	2672	2485	1000
IRMOF-2-Br	1722[11]	2693	329	2461	2206	882
IRMOF-2-I	1066[20]	2404	516	1911	1925	615
IRMOF-1	3800[9]	3187	3368			

^{a} All values reported have the units m^2/g. ^{b} Values were calculated using the Connolly method. See text. ^{c} See main text for a description of the activation procedure.
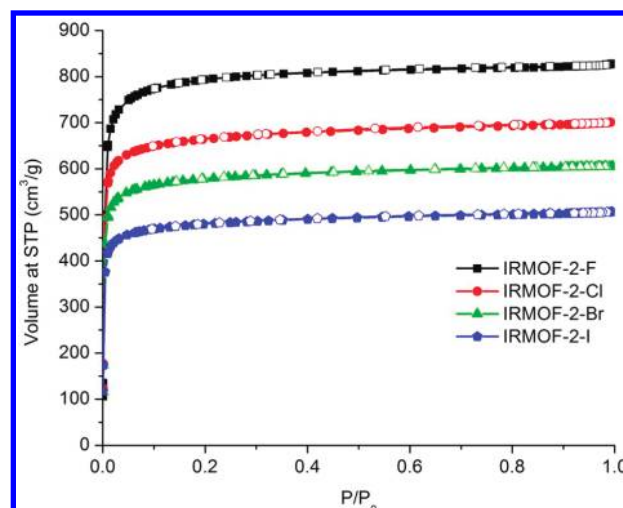

Figure 3. Nitrogen adsorption (solid) and desorption (open) isotherms for IRMOF-2-F, -Cl, -Br, and -I measured at 77 K and P_0 = 761.42 mmHg.

previously,[24] indicating that they are isostructural. Although IRMOF-2-I was recently reported,[20] no PXRD pattern or other structural characterization was included. While so far we were not able to obtain single crystals suitable for X-ray diffraction structural determination, unit cells indexed for single-crystal samples of IRMOF-2-F, IRMOF-2-Cl, and IRMOF-2-I all correspond to that of IRMOF-2, corroborating our structural assignment. For comparison, we also synthesized IRMOF-1, using the optimized procedure reported by Long and co-workers.[9]

As this IRMOF series represents a platform for probing the effects of polarizability, obtaining materials that closely match the crystallographic structure is crucial to making accurate comparisons

with model predictions. One method to confirm the crystallographic structure of a MOF is to measure the BET surface area. A low apparent surface area can indicate framework collapse or pore occlusion, either of which could affect adsorbate–framework interactions, although this might not be apparent from PXRD data. For IRMOF-1, a multitude of surface areas have been reported, with a correspondingly wide range of adsorption properties for these materials.[9] Similarly, reported surface areas for IRMOF-2-Br and IRMOF-2-I are substantially lower than values calculated using the Connolly surface method (as implemented in Material Studios), using a probe radius of 1.8 Å (Table 1). Thus, we explored several activation methods to maximize the surface areas of our MOFs, resulting in values that agree well with the predicted values.

Initially, we employed a modified version of the activation procedure reported by Long and co-workers.[9] Upon removal of MOF reaction mixtures from the oven, the DEF was decanted and replaced immediately with hot anhydrous DMF. Crystals were dislodged from the wall of the jar, and the DMF was decanted and replaced with fresh DMF. The solvent–crystal mixtures were then heated at 95 °C for 5 min and separated into three different portions. The first portion was soaked in anhydrous DMF for 6 days, with the solvent replaced on each of the first 3 days. These crystals were then soaked in anhydrous CHCl$_3$ for 6 days with a similar replacement regimen. The second and third MOF portions were soaked in anhydrous CHCl$_3$ and

Table 2. Pore Sizes of Halogenated MOFs[a]

MOF	calc[b] pore diameter (Å)	DA radius (Å)[c]	HK half pore width (Å)[c]	SF half pore width (Å)[c]	total pore volume (cm³/g)[d]
IRMOF-1	(15.0)[30]	8.8 (7.8[31])	4.3 (4.4)[29]	7.8	1.39 (1.19)[e]
IRMOF-2-F		9.0	3.9	7.3	1.28
IRMOF-2-Cl		8.8	3.9	7.0	1.09
IRMOF-2-Br	(12.8)[30]	8.8	3.9	6.8	0.94
IRMOF-2-I		8.7	3.9	6.6	0.77

[a] Values in parentheses were obtained from the literature. [b] Values calculated from crystallographic data. [c] Values for the halogenated IRMOF series were calculated from 77 K N_2 isotherms using Quantachrome QuadraWin software. [d] Total pore volume calculated at maximum adsorption using Quantachrome QuadraWin software. [e] Value calculated from crystallographic data.[32]

CH_2Cl_2, respectively, for 12 days, with the solvent replaced at similar intervals to the $DMF/CHCl_3$ activation. The MOF crystals were then evacuated at 10 mTorr at 125 °C for 14 h. We also tested supercritical CO_2 drying, which involves exchanging the MOF with dry EtOH, and then liquid CO_2, which is then heated under pressure to the supercritical phase. This technique, which is believed to eliminate the solvent surface tension, and thus prevent pore collapse, has been exploited to dramatically improve the apparent surface areas of MOFs that perform poorly with standard activation techniques.[10]

BET surface area measurements of these samples revealed that, for IRMOF-2-F, -Cl, and -Br, the extended $CHCl_3$ soak was most effective in activating the MOFs. For IRMOF-2-I, extended soaks in CH_2Cl_2 and $CHCl_3$ provided similar results. The values obtained (Table 1) compare favorably to predicted surface areas, and for IRMOF-2-Br and IRMOF-2-I, they substantially exceed those that appear in the literature. In all cases the methods involving an extended DMF soak and supercritical CO_2 drying gave lower surface areas. PXRD patterns of these samples show significant loss of crystallinity (see Supporting Information), indicating possible framework collapse due to instability during the extended DMF or EtOH soak. Heating the samples activated by supercritical CO_2 drying to 125 °C under vacuum did not appreciably increase their apparent surface areas.

The nitrogen adsorption isotherms at 77 K for the highest surface area materials in the halogenated MOF series appear in Figure 3. As expected for isostructural variants of IRMOF-1, they adhere to the type-I IUPAC classification, indicative of a microporous structure. Micropore analysis of these materials confirms this result. Pore size distributions were calculated for this series as well as for IRMOF-1 using the classical thermodynamic Dubinin–Astakhov (DA)[25] model as well as the semiempirical methods of Horvath–Kawazoe (HK)[26] and Saito–Foley (SF);[27] the results are listed in Table 2. These distributions all have a single narrow peak, suggesting a uniform pore size (see Supporting Information). In general, the pore size decreases slightly with increasing halogen size, although this effect is most pronounced with the SF analysis and least pronounced with HK, due to its assumption of slit-shaped pores. The pore radii obtained from the DA analyses are comparable to the DA radius reported for IRMOF-3 (8.5 Å)[28] and calculated for IRMOF-1 (8.8 Å). The HK half pore widths are smaller than those calculated and reported for IRMOF-1, 4.3 and 4.4 Å[29] respectively, as expected for these functionalized structures.

As a proof-of-concept test of the effects of linker polarizability on adsorbate interaction, we measured ambient temperature (292 K) nitrogen adsorption isotherms for the halogenated MOFs and IRMOF-1 from 0 to 760 mmHg. This temperature was chosen to
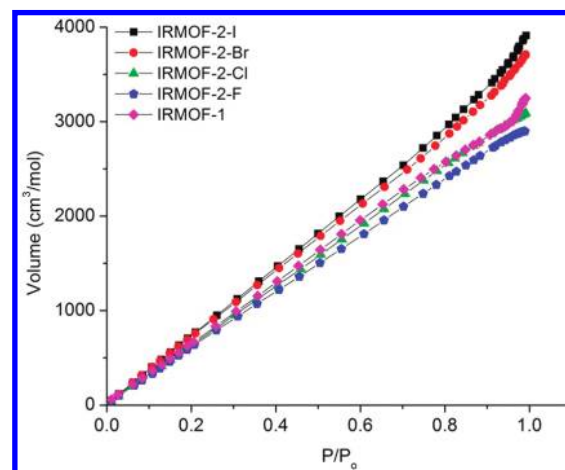

Figure 4. Nitrogen adsorption isotherms for IRMOF-2-F, -Cl, -Br, and -I measured at 292 K and P_0 = 760 mmHg.

more accurately reflect conditions used in separations and other industrial applications. Figure 4 shows that maximum nitrogen uptake per mole of MOF unit follows the trend -I > -Br > -Cl > -F, thus increasing with the increasing polarizability of the functional group. IRMOF-1, for comparison, has similar uptake to that of IRMOF-2-Cl.

In summary, we described the synthesis of the first isostructural MOF series with systematic −F, −Cl, −Br, and −I replacement. We also optimized the activation conditions, so that the surface areas of these materials now correlate well with values predicted computationally. This will minimize structural collapse and pore occlusion as confounding factors in exploration of their adsorption properties. The use of supercritical CO_2 drying does not lead to the highest surface areas, possibly due to framework instability in EtOH; the best results in the initial study of this method involved MOFs with very large pores. Finally, the measured ambient-temperature nitrogen adsorption isotherms accurately quantify the effects of linker polarizability, confirming the hypothesis that higher uptake is achieved as the functional group polarizability increases. The clear correlation established here will aid the process of synthetically tuning MOFs for specific adsorption applications, particularly those involving the uptake of weakly interacting gases.

■ ASSOCIATED CONTENT

Ⓢ Supporting Information. Experimental procedures for the synthesis and characterization of these materials, including

additional PXRD, NMR, and pore size distribution data. This material is available free of charge via the Internet at http://pubs.acs.org.

■ AUTHOR INFORMATION

Corresponding Author

*Telephone: 925-294-2895. E-mail: mdallen@sandia.gov.

■ ACKNOWLEDGMENT

■ REFERENCES

(1) Meek, S. T.; Greathouse, J. A.; Allendorf, M. D. *Adv. Mater.* **2011**, *23*, 249–267.

(2) Murray, L. J.; Dinca, M.; Long, J. R. *Chem. Soc. Rev.* **2009**, *38*, 1294–1314.

(3) Li, J. R.; Kuppler, R. J.; Zhou, H. C. *Chem. Soc. Rev.* **2009**, *38*, 1477–1504.

(4) Horcajada, P.; Chalati, T.; Serre, C.; Gillet, B.; Sebrie, C.; Baati, T.; Eubank, J. F.; Heurtaux, D.; Clayette, P.; Kreuz, C.; Chang, J. S.; Hwang, Y. K.; Marsaud, V.; Bories, P. N.; Cynober, L.; Gil, S.; Ferey, G.; Couvreur, P.; Gref, R. *Nat. Mater.* **2010**, *9*, 172–178.

(5) Lee, J.; Farha, O. K.; Roberts, J.; Scheidt, K. A.; Nguyen, S. T.; Hupp, J. T. *Chem. Soc. Rev.* **2009**, *38*, 1450–1459.

(6) Kobayashi, Y.; Jacobs, B.; Allendorf, M. D.; Long, J. R. *Chem. Mater.* **2010**, *22*, 4120–4122.

(7) Allendorf, M. D.; Houk, R. J. T.; Andruszkiewicz, L.; Talin, A. A.; Pikarsky, J.; Choudhury, A.; Gall, K. A.; Hesketh, P. J. *J. Am. Chem. Soc.* **2008**, *130*, 14404–14405.

(8) Kim, J.; Furukawa, H.; Ko, N.; Go, Y. B.; Aratani, N.; Choi, S. B.; Choi, E.; Yazaydin, A. O.; Snurr, R. Q.; O'Keeffe, M.; Yaghi, O. M. *Science* **2010**, *329*, 424–428.

(9) Kaye, S. S.; Dailly, A.; Yaghi, O. M.; Long, J. R. *J. Am. Chem. Soc.* **2007**, *129*, 14176–14177.

(10) Nelson, A. P.; Farha, O. K.; Mulfort, K. L.; Hupp, J. T. *J. Am. Chem. Soc.* **2009**, *131*, 458–460.

(11) Rowsell, J. L. C.; Yaghi, O. M. *J. Am. Chem. Soc.* **2006**, *128*, 1304–1315.

(12) Devic, T.; Horcajada, P.; Serre, C.; Salles, F.; Maurin, G.; Moulin, B.; Heurtaux, D.; Clet, G.; Vimont, A.; Greneche, J. M.; Le Ouay, B.; Moreau, F.; Magnier, E.; Filinchuk, Y.; Marrot, J.; Lavalley, J. C.; Daturi, M.; Ferey, G. *J. Am. Chem. Soc.* **2010**, *132*, 1127–1136.

(13) Achmann, S.; Hagen, G.; Kita, J.; Malkowsky, I. M.; Kiener, C.; Moos, R. *Sens.-Basel* **2009**, *9*, 1574–1589.

(14) Chen, B. L.; Yang, Y.; Zapata, F.; Qian, G. D.; Luo, Y. S.; Zhang, J. H.; Lobkovsky, E. B. *Inorg. Chem.* **2006**, *45*, 8882–8886.

(15) Deng, H. X.; Doonan, C. J.; Furukawa, H.; Ferreira, R. B.; Towne, J.; Knobler, C. B.; Wang, B.; Yaghi, O. M. *Science* **2010**, *327*, 846–850.

(16) He, M. Y.; Chen, S. C.; Zhang, Z. H.; Huang, K. L.; Yin, F. H.; Chen, Q. *Inorg. Chim. Acta* **2009**, *362*, 2569–2576.

(17) Jones, S. C.; Bauer, C. A. *J. Am. Chem. Soc.* **2009**, *131*, 12516–12517.

(18) Farha, O. K.; Malliakas, C. D.; Kanatzidis, M. G.; Hupp, J. T. *J. Am. Chem. Soc.* **2010**, *132*, 950–952.

(19) Furukawa, H.; Kim, J.; Ockwig, N. W.; O'Keeffe, M.; Yaghi, O. M. *J. Am. Chem. Soc.* **2008**, *130*, 11650–11661.

(20) Burrows, A. D.; Fisher, L. C.; Richardson, C.; Rigby, S. P. *Chem. Commun.* **2011**, *47*, 3380–3382.

(21) Uemura, T.; Ono, Y.; Hijikata, Y.; Kitagawa, S. *J. Am. Chem. Soc.* **2010**, *132*, 4917–4924.

(22) Hu, W.; Zhu, N. B.; Tang, W.; Zhao, D. H. *Org. Lett.* **2008**, *10*, 2669–2672.

(23) Kommeddy, A.; Bowsher, M. S.; Gunna, M. R.; Botha, K.; Vinod, T. K. *Tetrahedron Lett.* **2008**, *49*, 4378–4382.

(24) Eddaoudi, M.; Kim, J.; Rosi, N.; Vodak, D.; Wachter, J.; O'Keeffe, M.; Yaghi, O. M. *Science* **2002**, *295*, 469–472.

(25) Rouquerol, F.; Rouquerol, J.; Sing, K. In *Adsorption by Powders and Porous Solids*; Academic Press: London, 1999; pp 219–236.

(26) Horvath, G.; Kawazoe, K. *J. Chem. Eng. Jpn.* **1983**, *16*, 470–475.

(27) Saito, A.; Foley, H. C. *AlChE J.* **1991**, *37*, 429–436.

(28) Yoo, Y.; Varela-Guerrero, V.; Jeong, H. K. *Langmuir* **2011**, *27*, 2652–2657.

(29) Saha, D. P.; Wei, Z. J.; Deng, S. G. *Sep. Purif. Technol.* **2009**, *64*, 280–287.

(30) Pawsey, S.; Moudrakovski, I.; Ripmeester, J.; Wang, L. Q.; Exarhos, G. J.; Rowsell, J. L. C.; Yaghi, O. M. *J. Phys. Chem. C* **2007**, *111*, 6060–6067.

(31) Liu, Y. Y.; Ng, Z. F.; Khan, E. A.; Jeong, H. K.; Ching, C. B.; Lai, Z. P. *Microporous Mesoporous Mater.* **2009**, *118*, 296–301.

(32) Poirier, E.; Dailly, A. *J. Phys. Chem. C* **2008**, *112*, 13047–13052.

4312

dx.doi.org/10.1021/cg201136k |*Cryst. Growth Des.* 2011, 11, 4309–4312